Self-driven nonlinear dynamics in magneto-optical traps

T. Pohl
ITAMP, Harvard-Smithsonian Center for Astrophysics, 60 Garden Street, Cambridge, Massachusetts 02138, USA

G. Labeyrie and R. Kaiser
Institut Non Linéaire de Nice, UMR 6618, 1361 route des Lucioles, F-06560 Valbonne, France

(Received 7 February 2006; published 23 August 2006)

We present a theoretical model describing recently observed collective effects in large magneto-optically trapped atomic ensembles. Based on a kinetic description, we develop an efficient test particle method, which, in addition to the single-atom light pressure, accounts for other relevant effects such as laser attenuation and forces due to multiply scattered light with position-dependent absorption cross sections. Our calculations confirm the existence of a dynamical instability and provide deeper insights into the observed system dynamics.

DOI: 10.1103/PhysRevA.74.023409 PACS number(s): 32.80.Pj, 42.50.Vk, 47.35.−i, 52.35.−g

Since its first realization in 1987 [1], the magneto-optical trap (MOT) has become a standard technique for providing a robust source of large numbers of cold atoms. While multiple scattering of the absorbed laser light is known as a major limitation for achieving Bose-Einstein condensation, it also leads to interesting collective effects that have been studied over recent years [2–7], and a variety of static structures have been observed and investigated by different theoretical approaches [3,5,8–10].

Only recently, experiments have revealed a so far unexplored dynamical instability in three-dimensional MOTs connected with the appearance of self-excited radial oscillations [11], which constitutes a complex nonlinear dynamics phenomenon. Understanding the observed effect turns out to be of broader interest, as it shows close analogies to similar plasma and astrophysical phenomena, such as, e.g., pulsating stars [12].

Here we develop a theoretical model, describing the observed instability and providing a physical picture of the underlying mechanism. As discussed in [7], sub-Doppler cooling mechanisms only affect a very small fraction of large trapped atom clouds. Hence, the overall behavior of large atomic ensembles is well described within a basic Doppler-cooling picture, where the resulting trapping force along each laser beam can be written as [13,14]

$$F_{\mathrm{trap}}^{(i)}(x,v) = \frac{\hbar\Gamma}{2}[s_+\sigma_+(x,v) - s_-\sigma_-(r,v)], \tag{1}$$

where

$$\sigma_\pm = \sigma_0\left(1 + 3(s_+ + s_-) + 4\frac{(\delta \mp kv \mp \mu x)^2}{\Gamma^2}\right)^{-1} \tag{2}$$

is the absorption cross section for the two laser beams (including a saturation by the three pairs of laser beams), $\sigma_0 = 3\lambda/2\pi$ is the on-resonance absorption cross section, λ is the laser wavelength, Γ is the transition linewidth, δ is the detuning from resonance, μx determines the Zeeman shift of the atomic transition due to the MOT magnetic field, and $s_\pm = I_\pm / I_{\mathrm{sat}}$ denotes the saturation parameter of the respective laser beam of intensity $I_\pm$ with I_{sat} being the saturation intensity of the atomic transition. For the discussion below, it is convenient to split the force according to $F_{\mathrm{trap}}(x,v) = \alpha(|x|)x + \beta(|x|,|v|)v$, with $\alpha(|x|) = F_{\mathrm{trap}}(|x|,0)/|x|$ and $\beta(|x|,|v|) = [F_{\mathrm{trap}}(|x|,|v|) - F_{\mathrm{trap}}(|x|,0)]/|v|$.

In order to simplify our theoretical considerations, we use the following spherical symmetric generalization of Eq. (1):

$$\mathbf{F}_{\mathrm{trap}} = \alpha(r)\mathbf{r} + \beta(r,v)\mathbf{v}. \tag{3}$$

While experimental confinement configurations generally do not obey this symmetry, Eq. (3) describes the important features of the resulting force in both the linear and nonlinear trapping regions.

At higher densities, attenuation of the laser light inside the cloud results in an additional effective confining force experienced by the atoms [15]. To account for this effect within our spherical symmetry assumption, the spatial intensity profile is obtained from

$$s_+ = s_0 e^{-\int_r^\infty \sigma_+(r')\rho(r')}, \quad s_- = s_0 e^{-\int_0^\infty \sigma_+(r')\rho(r') - \int_0^r \sigma_-(r')\rho(r')}, \tag{4}$$

where s_0 is the saturation parameter of the incident beam. Moreover, multiple scattering of the absorbed laser light inside the cloud leads to an additional outward directed pressure, caused by an effective interaction between the atoms [2]. Neglecting higher-order scattering events, which are known to screen the atom-atom interaction [16], a photon scattered off an atom at position $\mathbf{r}_1$ exerts an average force on an absorbing atom at $\mathbf{r}_2$ according to [2,4]

$$\mathbf{F}_{\mathrm{rsc}} = \frac{3I_{\mathrm{sat}}}{4\pi c}(s_+\sigma_+\sigma_{\mathrm{rsc}}^{(+)} + s_-\sigma_-\sigma_{\mathrm{rsc}}^{(-)})\frac{\mathbf{r}_2 - \mathbf{r}_1}{|\mathbf{r}_2 - \mathbf{r}_1|^3}. \tag{5}$$

The reabsorption cross section $\sigma_{\mathrm{rsc}}^{(+/-)}$ is obtained by convolving the absorption cross section of the emitted light with the emission spectrum of the atom at r_1 in the presence of either left or right circularly polarized laser light. Note that σ_{rsc} may depend on both coordinates via the space dependence of the local laser intensities as well as of the respective detunings. Previously [3,4,7–10], such coordinate dependencies have been neglected, which, according to Eq. (5), results in a

Coulomb-like interaction with effective charges, again underlining the close analogy with plasma and gravitational physics problems. In large clouds, however, we find the position dependence of the effective charges to be important for the static and dynamics properties of the trapped atom cloud.

Starting from Eqs. (2)–(5), the collective system dynamics is described by the following kinetic equation:

$$\frac{\partial f}{\partial t} + \mathbf{v}\frac{\partial f}{\partial \mathbf{r}} + M^{-1}\alpha(r)\mathbf{r}\frac{\partial f}{\partial \mathbf{v}} + M^{-1}\mathbf{F}_{\mathrm{mf}}(\mathbf{r})\frac{\partial f}{\partial \mathbf{v}} + M^{-1}\frac{\partial}{\partial \mathbf{v}}[\mathbf{v}\beta(r,v)f] = 0 \tag{6}$$

for the atomic phase-space density $f(\mathbf{r},\mathbf{v},t)$, where

$$\mathbf{F}_{\mathrm{mf}}(\mathbf{r}) = \int \mathbf{F}_{\mathrm{rsc}}(\mathbf{r}',\mathbf{r})f(\mathbf{r}',\mathbf{v})d\mathbf{v}d\mathbf{r} \tag{7}$$

and M is the mass of the atoms. Heating by spontaneous emission and photon exchange [16,17] has been neglected, since for the densities considered in this work the corresponding thermal pressure is much smaller than the pressure resulting from the effective atomic repulsion.

Note that Eq. (7) goes beyond a local-density approximation [16], retaining the complete position dependence of σ_{rsc} and the density dependence of $\mathbf{F}_{\mathrm{rsc}}$. In fact, this nonlocal space dependence of all forces in Eq. (6) in addition to their local dependence on the atom position render a direct numerical solution of Eq. (6) very demanding. Alternatively, we apply an efficient numerical procedure based on a test-particle treatment, similar to particle-in-cell methods [18], frequently used for plasma physics problems. More specifically, we represent the atomic density by an ensemble of $N_t < 10^6$ test particles, whose number is typically chosen to be less than the actual particle number to reduce the numerical effort. The respective absorption cross sections and masses of the test particles are adjusted, such that the results are independent of the number N_t of test particles. By propagating every particle according to the forces Eqs. (3) and (7), we obtain the time-dependent density from which we calculate the local intensities and the resulting forces to advance the next time step.

To study its stationary properties, we evolve the atomic cloud until it relaxes to the self-consistent, stationary solution of Eq. (6), which we found to exist only below a critical atom number N_c. Figure 1(a) shows the calculated stationary density profile for $N=1.15\times10^9$ rubidium atoms and typical MOT parameters of $I=1.0\ \mathrm{mW/cm^2}$, $\delta=-1.5\Gamma$, and $\Gamma/\mu=4.7$ mm (corresponding to 9 G/cm) [11]. As can be seen, the calculated density is well described by a truncated Gaussian profile. As the atom number is decreased, the truncation radius R decreases relative to the rms width of the corresponding Gaussian, ultimately leading to a transition into a uniform density profile. Similar changes in the density profile have also been reported in MOTs, where the nonlinearity of the potential arises from sub-Doppler trapping mechanisms [7,19]. In the present case, the observed transition results from the nonlinearity and the position dependence of the reabsorption cross section and, hence, cannot be found under the assumption of linear trapping forces and pure Coulomb-like interactions [3,4,10].

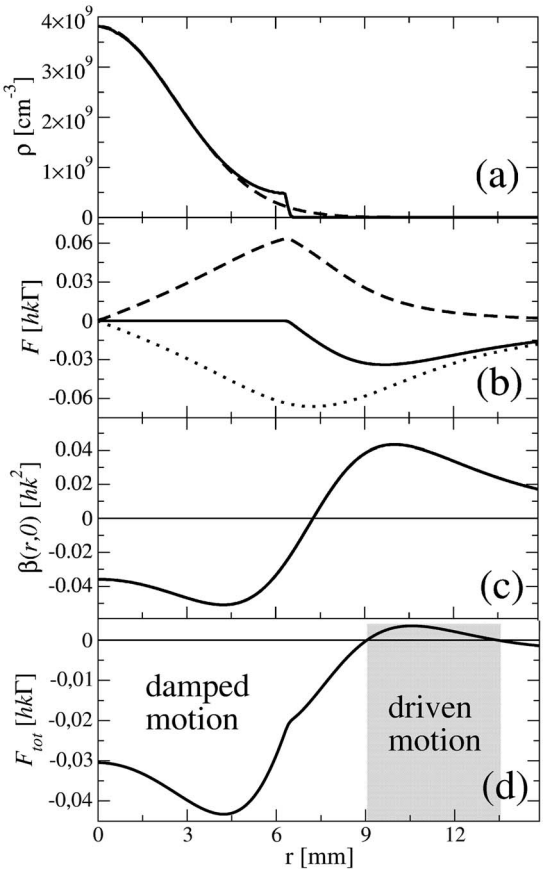

FIG. 1. (a) Radial density profile (solid line) of trapped rubidium atoms with $\delta=-1.5\Gamma$, $I=1.0$ mW/cm, and $\Gamma/\mu=4.7$ mm together with a Gaussian fit (dashed line). (b) Radial dependence of F_{mf} (dashed line), F_{trap} (dotted line), and $F_{\mathrm{mf}}+F_{\mathrm{trap}}$ (solid line). (c) Radial dependence of the damping constant $\beta(r,v=0)$. (d) Radial dependence of the total force on an outward moving atom with velocity $0.85\Gamma/k$. The gray shaded area marks the region of active atomic motion.

Let us now turn to the most striking result of our calculations. As we increase further the number N of atoms, the cloud becomes unstable at a critical atom number N_c, corresponding to a critical radius R_c. By varying the various MOT parameters, we find that the critical radius is uniquely determined by the relation $R_c=\delta/\mu$ [see Fig. 3(a)], confirming the conclusion reached in [11]. This fact is illustrated in Figs. 1(b)–1(d), where we show the radial dependence of the trapping and interaction force as well as the damping constant $\beta(r,v=0)$. The damping constant $\beta(r,0)$ reverses its sign at $R_c=\delta/\mu$. Hence, any small velocity of atoms outside of R_c will be enhanced. While inward-moving particles will be damped again when entering the negative-β region, outward-moving atoms around R_c are further accelerated away from the trap center, since the single-atom light pressure force is largely balanced by the interaction force around $r=R_c$. Their motion around the fixed point ($r=R_c$, $v=0$) will become unstable and limited by the nonlinear terms of the force. At

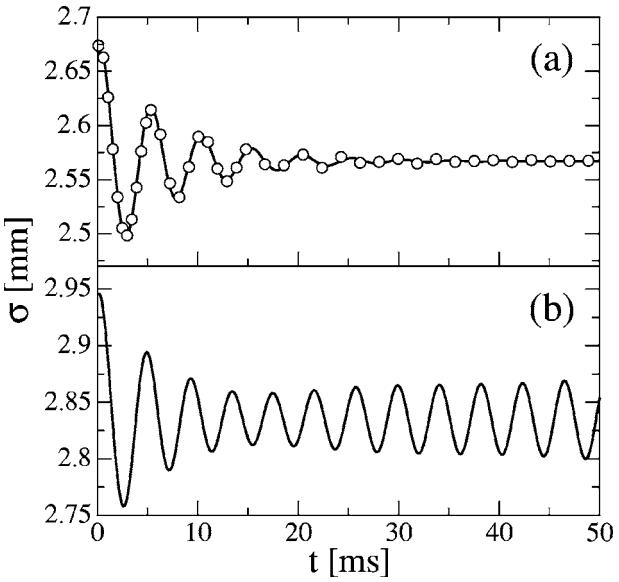

FIG. 2. Relaxation of the MOT's rms radius after switching the detuning from $\delta_0=-1.55\Gamma$ to $\delta=-1.5\Gamma$ for two different particle numbers of $N=9\times10^8$ (a) and $N=1.3\times10^9$ (b). The remaining parameters are the same as in Fig. 1. The solid line in (a) shows a fit of $\Delta\sigma\sin(\omega t+\phi)e^{-t/\tau}+\sigma_\infty$ to the numerical data (circles). The solid line in (b) shows the numerical data in the oscillating regime of $N>N_c$.

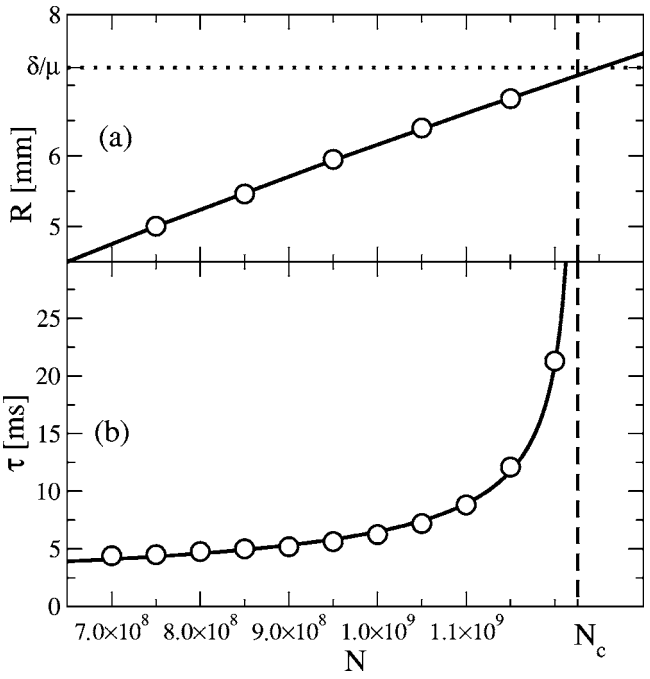

FIG. 3. (a) Calculated MOT size as a function of the atom number (circles) fitted by a power-law dependence (solid line). The dotted line corresponds to the critical radius $R_c=\delta/\mu$ and the dashed line in both figures indicates the critical atom number N_c beyond which the dynamical instability sets in. (b) Real part of the MOT's stability coefficient (circles) fitted by $\tau\propto(N-N_c)^\kappa$ with $N_c=1.226\times10^9$ and $\kappa=0.55$.

larger distances, however, the total force reverses its sign again, since the interaction force decreases much more rapidly than the trapping, due to the radially increasing Zeeman shift [see Fig. 1(b)]. As shown in Fig. 1(d), this leads to the formation of a finite active region, similar to theoretical descriptions of pulsating stars [12], feeding the oscillatory dynamics of the MOT. Note that in previous models with position-independent reabsorption cross sections, the active region would extend to infinity and the atoms would be simply spilled out of the MOT region. Hence, if during the expansion the atoms do not acquire a velocity beyond the capture range of the MOT, a stable limit cycle will be reached.

In order to characterize the onset of the instability, we analyze the cloud's rms radius $\sigma=\sqrt{\langle r^2\rangle/3}$ and study its sensitivity against a small perturbation. More precisely, we start from a stationary density corresponding to some detuning δ_0, which is instantly increased to δ (closer to resonance), leading to damped oscillations of σ toward its new equilibrium value σ_∞, as shown in Fig. 2(a). From a fit to a damped harmonic oscillation $\sigma=\Delta\sigma e^{-t/\tau}\sin(\omega t+\phi)+\sigma_\infty$, we obtain the damping time τ and frequency ω corresponding to the real and imaginary part of the respective Lyapunov exponent $\lambda=\tau^{-1}+i\omega$ [Fig. 3(b)]. For increasing N and the parameters of Fig. 2, the instability sets in at an atom number of $N_c=1.226\times10^9$ and with a critical exponent of 0.55. On the other hand, the frequency of the cloud oscillation evolves continuously through the instability threshold (see Fig. 2), indicating that the onset of the instability proceeds via a supercritical Hopf bifurcation.

A reduction of the system properties to a single quantity like the cloud's rms radius is clearly helpful for understanding the transition into the oscillating regime. On the other hand, the fully resolved space-time evolution of the atomic density such as shown in Fig. 4 reveals much more detailed information about the complicated dynamics of the cloud. Indeed, the complex density patterns at larger atom numbers (see Fig. 4) show that the oscillation dynamics is much more complex than a simple breathing mode, as suggested by the simple size oscillations close to the instability threshold [see Fig. 2(b)].

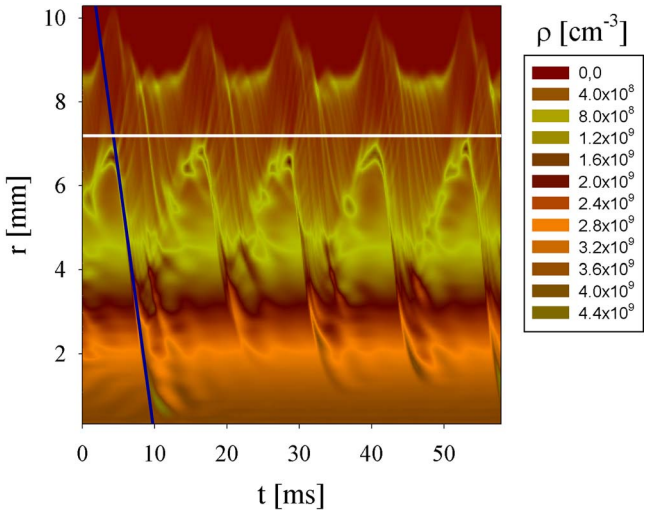

FIG. 4. (Color online) Spatio-temporal evolution of the atomic density for $N=1.7\times10^9$. The MOT parameters are the same as in Fig. 1. The lines are discussed in the text.

In fact, the oscillation is triggered by an outer fraction of atoms, which gain energy as they move in and out of the active region of $r > R_c$, which is indicated by the horizontal white line in Fig. 4. When bouncing back on the low-energetic atoms, the gained energy is deposited by exciting a density wave just inside the region with $\beta(r,0) < 0$. Subsequently, the formed nonlinear excitation propagates toward the trap center along the diagonal blue line drawn in Fig. 4 thereby losing energy, mostly due to the damping by the cooling lasers. As can be seen in Fig. 4, this not only leads to a flattening and broadening of the density wave until it disappears, but also to a deceleration as indicated by the deviation of the moving maximum from the blue line at smaller distances. At the same time, the edge region of the atomic cloud starts to relax, causing some atoms to be again accelerated away from the center and the whole process repeats itself. Although this scenario clearly provides the basic mechanism for the observed oscillations, our calculations reveal a complex nonlinear dynamics with a number of finer details (see Fig. 4).

In conclusion, large clouds of magneto-optical confined atoms have been found to exhibit a very complex nonlinear dynamics. Our theoretical description has revealed the onset of a deterministic instability connected with self-sustained oscillations in agreement with recent experiments [11]. It has been found that a number of different effects, such as the attenuation of the trap lasers, rescattering of the absorbed laser light, and, equally important, the position dependence of the respective absorption cross sections are *all* necessary to explain the observed phenomenon. A stability analysis of the MOT size has shown that the transition proceeds via a supercritical Hopf bifurcation. The obtained density evolution revealed the build-up of complex nonlinear excitations driven by the combined action of the light-pressure force and the effective atomic interaction, which results in an active atomic motion at large distances. Similar types of active or self-driven motion are currently being discussed in a broad range of different applications, such as collective swarm dynamics [20], propagation of waves [21] or dissipative solitons [22] in reaction-diffusion systems, or grain motion in dusty plasmas [23]. Hence, we believe that large clouds of magneto-optical confined atoms provide an ideal laboratory system for further exploration of the rich spectrum of self-driven motion, including variable system geometries, effects of external driving, and possibilities to control the system dynamics.

T.P. would like to acknowledge the kind hospitality during a stay at the Institut Non Linéaire de Nice, where major parts of the work have been performed, and also the support from the ESF through the Short Visit Grant No. 595 and from the NSF through a grant for the Institute of Theoretical Atomic, Molecular and Optical Physics (ITAMP) at Harvard University and Smithsonian Astrophysical Observatory.

[1] E. L. Raab, M. Prentiss, A. Cable, S. Chu, and D. E. Pritchard, Phys. Rev. Lett. **59**, 2631 (1987).
[2] T. Walker, D. Sesko, and C. Wieman, Phys. Rev. Lett. **64**, 408 (1990).
[3] D. Sesko, T. Walker, and C. Wieman, J. Opt. Soc. Am. B **8**, 946 (1991).
[4] A. M. Steane, M. Chowdhury, and C. J. Foot, J. Opt. Soc. Am. B **9**, 2142 (1992).
[5] V. S. Bagnato, L. G. Marcassa, M. Oria, G. I. Surdutovich, R. Vitlina, and S. C. Zilio, Phys. Rev. A **48**, 3771 (1993).
[6] M. T. de Araujo, L. G. Marcassa, S. C. Zilio, and V. S. Bagnato, Phys. Rev. A **51**, 4286 (1995).
[7] C. G. Townsend, N. H. Edwards, C. J. Cooper, K. P. Zetie, C. J. Foot, A. M. Steane, P. Szriftgiser, H. Perrin, and J. Dalibard, Phys. Rev. A **52**, 1423 (1995).
[8] L. Pruvost, I. Serre, H. T. Duong, and J. Jortner, Phys. Rev. A **61**, 053408 (2000).
[9] R. S. de Oliveira, E. P. Raposo, and S. S. Vianna, Phys. Rev. A **70**, 023402 (2004).
[10] A. S. Arnold and P. J. Manson, J. Opt. Soc. Am. B **17**, 497 (2000).
[11] G. Labeyrie, F. Michaud, and R. Kaiser, Phys. Rev. Lett. **96**, 023003 (2006).
[12] J. P. Cox, *Theory of Stellar Pulsation* (Princeton University Press, Princeton, NJ, 1980).
[13] P. D. Lett, W. D. Phillips, S. L. Rolston, C. E. Tanner, R. N. Watts, and C. I. Westbrook, J. Opt. Soc. Am. B **6**, 2084 (1989).
[14] H. J. Metcalf and P. van der Straten, *Laser Cooling and Trapping* (Springer, New York, 1999).
[15] J. Dalibard, Opt. Commun. **68**, 203 (1988).
[16] K. Ellinger, J. Cooper, and P. Zoller, Phys. Rev. A **49**, 3909 (1994).
[17] A. M. Smith, K. Burnett, and J. Cooper, Phys. Rev. A **46**, 4065 (1992).
[18] C. K. Birdsall and A. B. Langdon, *Plasma Physics via Computer Simulation* (Adam Hilger, New York, 1991).
[19] J. W. Jun, S. Chang, T. Y. Kwon, H. S. Lee, and V. G. Minogin, Phys. Rev. A **60**, 3960 (1999).
[20] U. Erdmann, W. Ebeling, and A. S. Mikhailov, Phys. Rev. E **71**, 051904 (2005).
[21] T. Sakurai, E. Mihaliuk, F. Chirila, and K. Showalter, Science **296**, 2009 (2002).
[22] H. U. Bödeker, M. C. Röttger, A. W. Liehr, T. D. Frank, R. Friedrich, and H.-G. Purwins, Phys. Rev. E **67**, 056220 (2003).
[23] S. A. Trigger, Phys. Rev. E **67**, 046403 (2003).